THE GEOLOGICAL SOCIETY OF AMERICA®

Temperature and volume of global marine sediments

Douglas E. LaRowe[1], Ewa Burwicz[2], Sandra Arndt[3], Andrew W. Dale[2], and Jan P. Amend[1,4]
[1]Department of Earth Sciences, University of Southern California, Zumberge Hall of Science, 3651 Trousdale Parkway, Los Angeles, California 90089, USA
[2]GEOMAR Helmholtz Centre for Ocean Research, Wischhofstraße 1-3, 24148 Kiel, Germany
[3]School of Geographical Sciences, University of Bristol, University Road, Bristol BS8 1SS, UK
[4]Department of Biological Sciences, University of Southern California, 3616 Trousdale Parkway, AHF 107, Los Angeles, California 90089, USA

ABSTRACT

Marine sediments contribute significantly to global element cycles on multiple time scales. This is due in large part to microbial activity in the shallower layers and abiotic reactions resulting from increasing temperatures and pressures at greater depths. Quantifying the rates of these diagenetic changes requires a three-dimensional description of the physiochemical properties of marine sediments. In a step toward reaching this goal, we have combined global data sets describing bathymetry, heat conduction, bottom-water temperatures, and sediment thickness to quantify the three-dimensional distribution of temperature in marine sediments. This model has revealed that ~35% of sediments are above 60 °C, conditions that are suitable for petroleum generation. Furthermore, significant microbial activity could be inhibited in ~25% of marine sediments, if 80 °C is taken as a major thermal barrier for subsurface life. In addition to a temperature model, we have calculated new values for the total volume (3.01 × 10^8 km^3) and average thickness (721 m) of marine sediments, and provide the only known determination of the volume of marine-sediment pore water (8.46 × 10^7 km^3), equivalent to ~6.3% of the volume of the ocean. The results presented here can be used to help quantify the rates of mineral transformations, lithification, catagenesis, and the extent of life in the subsurface on a global scale.

INTRODUCTION

The regular delivery of organic and inorganic matter to the seafloor results in a stratigraphic accumulation of biological and geological material that can be used to infer Earth's history. However, marine sediments are not simply passive recorders of a changing planet. Processes occurring in sediments can affect the various sets of isotopic, biogenic and/or authigenic mineral and biomarker data that are used to interpret paleoenvironmental records (Zonneveld et al., 2010). In the upper tens of centimeters of sediments, the relatively vigorous microbial oxidation of organic carbon alters the saturation state of pore waters with respect to calcium carbonate minerals, and thus their burial, an important part of the Walker thermostat that keeps Earth's temperature within livable limits (Emerson and Bender, 1981; Walker et al., 1981). In addition, organic matter degradation is coupled to Fe, Mn, and S cycles (e.g., Jørgensen, 1982; Van Cappellen and Wang, 1996), and abiotic reactions can modify the fabric and composition of marine sediments as some minerals dissolve and others precipitate. Whether the processes are biologically mediated or completely abiotic, near the sediment-water interface (SWI) or several kilometers below it, temperature is a master variable that influences diagenesis. To better understand the effect of the biogeochemical evolution of marine sediments, a robust quantitative description of the physical properties of these sediments is required.

METHODS

We divided the ocean floor into three domains, shelf, margin, and abyss, in order to fully parameterize the model described here. This was done because some of the parameters describing sediments are not well constrained on a global basis (Table 1; see Fig. DR1 in the GSA Data Repository[1]). Although this is a rough approximation for environmental variability across sedimentary basins, it nonetheless captures broad variations and provides a robust quantitative estimation of marine sediment properties on a global scale. The location of the continental margin boundaries was adopted from Vion and Menot (2009): shelf environments roughly correspond to water depths <200 m, with the exception of the Antarctic region, where these areas correspond to water depths <500 m, and areas deeper than ~3500 m are the abyssal plain. The remainder, the margin, corresponds to the continental rise and slope. Within these definitional constraints, continental shelf underlies ~6.33% of ocean surface area, margins make up 10.78%, and the abyssal domain constitutes the remaining 82.89% (see Fig. DR1).

The porosities (ϕ) of marine sediments in the shelf, margin, and abyss domains were calculated as a function of depth in meters (z) using a formulation commonly used in basin- to global-scale studies (Athy, 1930):

$$\phi_{(z)} = \phi_0 \exp(-c_0 z), \tag{1}$$

where ϕ_0 denotes the porosity at the SWI and c_0 (m^{-1}) stands for the compaction length scale, which characterizes how a given sediment type will compact under its own weight. Values of ϕ_0 and c_0 were chosen to describe the shelf, margin, and abyss based on sediments that are representative of these domains (Hantschel and Kauerauf, 2009) (see Table 1). Global sediment thickness data available at 5′ × 5′ resolution (Divins, 2003; Laske and Masters, 1997; Whittaker et al., 2013) were resampled using a spline interpolation into a 0.25° × 0.25° grid. The volume of marine sediments was extracted from the resulting global sediment thickness map.

TABLE 1. SELECTED VALUES OF PARAMETERS USED TO CHARACTERIZE THE TEMPERATURE AND POROSITY OF CONTINENTAL SHELF, CONTINENTAL MARGIN, AND ABYSS DOMAINS OF GLOBAL MARINE SEDIMENTS

Parameter	Definition	Shelf	Margin	Abyss	Units
ϕ_0	sediment porosity at the sediment-water interface	0.45*	0.74*,†	0.70*	(–)
c_0	sediment compaction length scale	0.5 × 10^{-3}*	1.7 × 10^{-3}*,†	0.85 × 10^{-3}*	m^{-1}
λ_s	thermal conductivity of sediment grains	3.2*	2.5*,†	1.7*	W m^{-1} K^{-1}

*These values are representative of a sandstone-siltstone mixture (shelf), a sandstone-siltstone- shale combination (margin) and typical shales and biogenic-dominated sediments (abyss) (Hantschel and Kauerauf, 2009).
†Wallmann et al. (2012)

[1]GSA Data Repository item 2017072, Figure DR1 (map of the three domains in this study), Figure DR2 (summary of the methods section in the main text in a single image), and Figure DR3 (volume of pore water in marine sediments at particular temperature intervals), is available online at www.geosociety.org/datarepository/2017, or on request from editing@geosociety.org.

Pore-water volume was derived from depth-integrated porosity profiles calculated from Equation 1. Integration of these properties accounted for the differential surface area of each 0.25° × 0.25° grid cell according to their latitude and longitude.

The steady-state depth-temperature profile of marine sediments [$T_{(z)}$] was calculated using

$$T_{(z)} = T_{\mathrm{SWI}} + \frac{q \cdot z}{\lambda_{\mathrm{b}(z)}}, \quad (2)$$

where T_{SWI} stands for the temperature (K) at the SWI, q represents heat flow (W m^{-2}), and $\lambda_{\mathrm{b}(z)}$ refers to the thermal conductivity (W m^{-1} K^{-1}) of bulk sediment. Values of T_{SWI} are equal to bottom-water temperatures extracted from the ORCA-R025 (Barnier et al., 2006) configuration for an ocean general circulation model at 0.25° × 0.25° resolution. Irregular heat-flow data from the International Heat Flow Commission were extrapolated to a 0.25° × 0.25° grid using a spherical harmonics analysis (Hamza et al., 2008). In order to represent how variable porosity and mineralogy affect the thermal conductivity of marine sediments, values of $\lambda_{\mathrm{b}(z)}$ were calculated using the geometric mean of the thermal conductivities of pore fluid and sediment grains (Fuchs et al., 2013):

$$\lambda_{\mathrm{b}(z)} = \lambda_{\mathrm{s}}^{(1-\phi)} \cdot \lambda_{f}^{\phi}, \quad (3)$$

where λ_{s} and λ_{f} refer to the thermal conductivity of sediment grains and pore fluids, respectively [λ_{f} = 0.6 W m^{-1} K^{-1} for all domains (Castelli et al., 1974); see Table 1 for values of λ_{s}]. The global volume of sediments in different temperature intervals was calculated by integrating the results of Equation 2 in combination with the sediment thickness data. Advection of temperature with sediment burial was shown to be negligible, and therefore not explicitly accounted for. See Figure DR2 for a workflow view of the methods outlined here.

The sensitivity of the model results was tested with alternative values of the parameters given in Table 1. For total fluid volume, we used different combinations of ϕ_0 and c_0 that are ±10% of those given in Table 1. Similarly, the volumes of sediment within discrete temperature intervals were calculated using values of λ_{s} that are ±10% of those given in Table 1 along with the values of ϕ_0 and c_0 given in Table 1.

RESULTS

Equations 1–3 and the parameter values given in Table 1 were used to calculate the spatial distribution of temperature in marine sediments. The results, depicted in Figure 1, show the thickness of sediment that is within particular temperature ranges (e.g., 0–20 °C). It should be noted that the sediment thickness scales for the panels in Figure 1 differ substantially. In Table 2, we report the global volumes of sediments at discrete temperature intervals and the variations in these volumes if different values of thermal conductivities of sediment grains (λ_{s}) are used. Note that 24.8% of the world's marine sediments are at 0–20 °C, 16.5% are at 40–60 °C, and 24.7% are above 80 °C. If values of λ_{s} are 10% higher than those listed in Table 1, then the proportion of sediments that are above 60 °C decreases relative to the baseline case. The opposite trend is seen when values of λ_{s} are 10% lower. The deepest and therefore the hottest sediments (>120 °C) undergo the largest total volume differences (+22.8% and −18.2%) when λ_{s} values are ±10% of those given in Table 1. This is due to the fact that deep sediments are largely devoid of pore space and, as a result, their thermal conductivity is dominated by that of the sediment grains.

The total global volume of marine sediments is calculated to be 3.01 × 10^8 km^3, resulting in an average thickness of 721 m (maps showing the volumes of pore water in discrete temperature intervals are shown in Fig. DR3). The sediments are not, however, distributed equally; >73% (2.22 × 10^8 km^3) are within 500 km of the coast. The sediment thickness data were

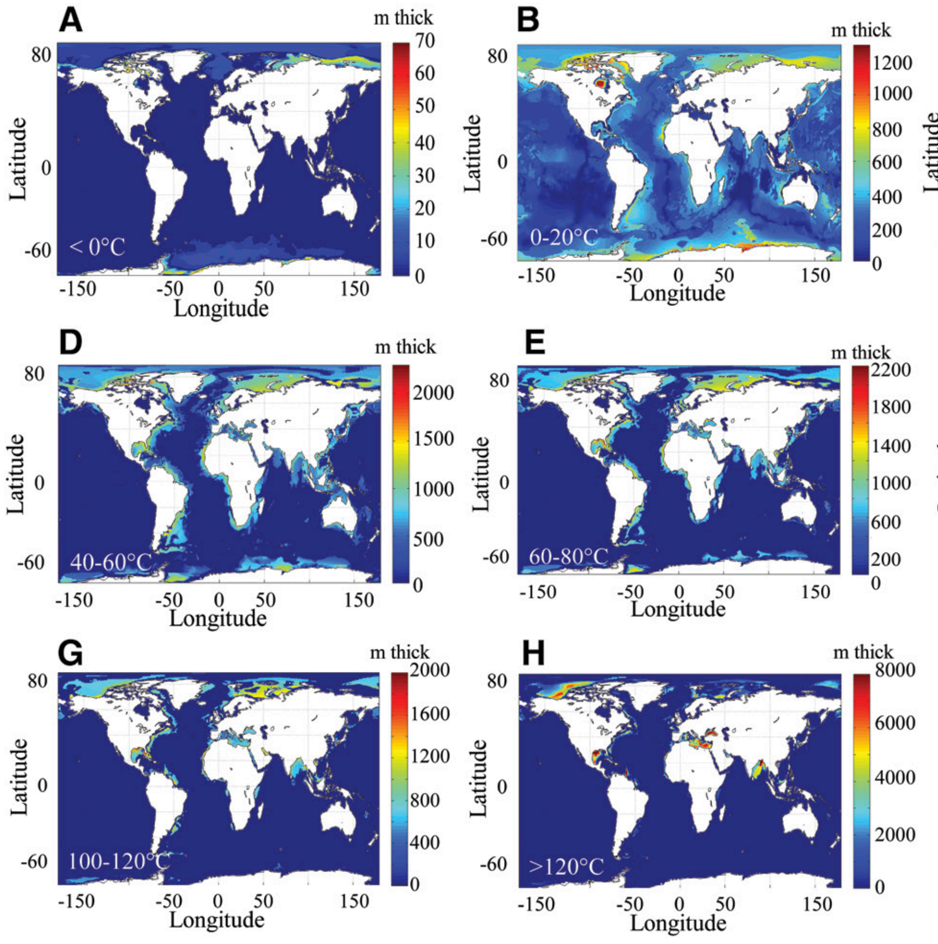

Figure 1. Global distribution of temperature in marine sediments. In each panel, the thickness of marine sediments within the indicated temperature range is given for a particular grid cell. Note that the scale, and therefore the color palette, for each panel is different, especially that for the coldest (<0 °C) and hottest sediments (>120 °C), A and H, respectively.

TABLE 2. VOLUMES OF OCEAN SEDIMENTS AT VARIOUS TEMPERATURE INTERVALS AND PERCENT CHANGES OF THESE VOLUMES ASSOCIATED WITH VARYING VALUES OF THE THERMAL CONDUCTIVITIES OF SEDIMENT GRAINS, λ_S, IN TABLE 1 BY ±10%

Temperature (°C)	Volume (km^3)	total (%)	Volume change (%)	
			–10% λ_s	+10% λ_s
< 0	2.59×10^5	0.1	–5.8	+ 5.0
0–20	7.46×10^7	24.8	–5.9	+ 5.9
20–40	6.96×10^7	23.2	–7.3	+ 6.7
40–60	4.95×10^7	16.5	–3.2	+ 1.8
60–80	3.20×10^7	10.7	+ 1.6	–2.5
80–100	2.10×10^7	6.9	+ 4.8	–5.2
100–120	1.47×10^7	4.9	+ 6.1	–6.8
>120	3.90×10^7	12.9	+ 22.8	–18.2
Total	3.01×10^8	100		

combined with the porosity model summarized by Equation 1, the three-domain model for ocean provinces described above, and the parameters listed in Table 1 to estimate that marine sediments contain 8.46×10^7 km³ (+15.6%/–14.1%) of water. In the sensitivity tests, a combination of low seafloor porosity (–10% ϕ_0) and high compaction length scale (+10% c_0) resulted in a maximum total decrease of pore-fluid volume of ~14.1%. However, high ϕ_0 (+10%) and low c_0 (–10%) parameters led to a total pore-fluid volume 15.6% larger than the baseline estimate.

DISCUSSION

Temperature influences the thermodynamic tendency of reactions to happen, the kinetics of these reactions, the diffusion of chemical species, and the density and viscosity of water. By determining the three-dimensional distribution of temperature of marine sediments, it has become possible to start to quantitatively address global-scale diagenesis, catagenesis, and the limits of life in the subsurface. For example, as temperatures approach and exceed 100 °C, some clay minerals reorganize into other clay types (Prothero and Schwab, 2004), a situation that could exist in nearly 18% of marine sediments (see Table 2). Other sediment lithification reactions, which include the dissolution and precipitation of mineral grains, can be accelerated by increasing temperature, and result in porosity and permeability decreases while altering pore-fluid chemistry. The evolution of the clay mineral smectite provides an instructive example of how, in addition to temperature, a suite of physiochemical properties influences its diagenesis (e.g., Aagaard and Helgeson, 1983; Kastner et al., 1991). Smectite tends to dehydrate when subjected to increasing pressure, but the degree to which this happens also depends on temperature, the identities of interlayer cations, and the concentrations of cations present in solution (Ransom and Helgeson, 1995). Because there is a positive volume change associated with its dewatering, with the right combination of pressure, temperature, and composition, tectonic events could result in a rapid dehydration event sending a pulse a fluid along a fault plane. This would also have the effect of depressing the local geothermal gradient temporarily while potentially sending election donors and/or acceptors from one part of a sedimentary package into another.

Similarly, the composition of marine sediments can be transformed through the abiotic conversion of organic carbon into petroleum: the principle zone of catagenesis occurs from ~50 to 160 °C, with pressure playing a lesser role (Tissot and Welte, 1984). As noted here, ~35% of marine sediments are above 60 °C, and even if sediments contain minimal organic matter, the complex organic matter in them can still be converted to microbially edible hydrocarbons through abiotic processes (Horsfield et al., 2006).

Although there are many factors that determine the habitability of a given environment, one of the most critical is temperature. The amount of energy that microorganisms require to maintain their structural and chemical integrity increases with temperature (Harder, 1997). In addition, the rates of abiotic redox reactions generally speed up as temperature increases, thus depriving microorganisms of the disequilibrium that is needed to gain energy. As a result of increased energetic and physiochemical stresses accompanying higher temperatures, the thermal limit for microorganisms in marine sediments is likely to be considerably lower than that established in the laboratory, 122 °C (Takai et al., 2008). It has been noted that biotic activity is extremely limited in natural environments at temperatures above ~80 °C (Head et al., 2014; Röling et al., 2003; Wilhelms et al., 2001), and consequently ~25% of marine sediments would be off limits for life. However, this leaves nearly 2.30×10^8 km³ of marine sediments habitable. If the maximum were 60 °C, then the hospitable volume would drop to 2.01×10^8 km³. By comparison, Lipp et al. (2008) estimated that the habitable volume of marine sediments is ~1.9×10^8 km³, but they partitioned the seafloor into 2 domains, used a single global geotherm (30 °C/km), and set a thermal limit for life equivalent to 3000 m below the SWI. (It is unclear what bottom-water temperature they used and therefore what the associated temperature limit is.)

The global volume of marine sediments calculated here, 3.01×10^8 km³, is about one-third smaller than that of the only other published value that we could find in the literature (4.5×10^8 km³) (Kennett, 1982). A critical comparison of the two estimates is precluded because the source of the previous literature value was given only as a personal communication. However, this massive number can be compared to the global volume of seawater, 1.335×10^9 km³, which is only 4.4× the volume of marine sediments. Although marine sediments are very unevenly distributed, this volume and surface area of the ocean can be combined to yield an average global sediment thickness of 721 m. This new estimate is ~69% thicker than other commonly cited estimates (e.g., 500 m; Fowler, 1990). The average thickness of shelf, margin, and abyss sediments are 250 m, 2270 m, and ~545 m, respectively. Other estimates of sediment thickness for the continental margin (1952 m) and open ocean (416 m) (Lipp et al., 2008) are difficult to compare to those reported here because, as noted here, Lipp et al. (2008) used other methods and data sets.

If all marine sedimentary pore space is occupied by water, then there would be 8.46×10^7 km³ (+15.6%/–14.1%) of pore fluid. This is ~6% of the global ocean, more than the Southern Ocean (7.18×10^7 km³) and 4.5 times that of the Arctic Ocean (1.88×10^7 km³) (Eakins and Sharman, 2010). The marine sediment pore-water volume is thus more than 3 times greater than that of the free water thought to fill the void spaces in the global igneous ocean aquifer (2.6×10^7 km³) (Johnson and Pruis, 2003), and ~3.7× the volume of groundwater in the upper 2 km of continental crust (2.26×10^7 km³) (Shiklomanov, 1993). To our knowledge, no estimates of this quantity have been published in the literature, but the repercussions of including this reservoir in the global hydrological cycle could be profound because it is compositionally distinct from ocean water, typically enriched in volatiles, trace elements, alkalinity, and dissolved inorganic carbon (Deyhle and Kopf, 2001). Significant quantities of sedimentary pore water are released into the ocean every year through active mud volcanoes (Dimitrov, 2002; Milkov, 2000), which have been observed on continental shelves, continental slopes, and the abyssal plains of inland seas, and number between 1000 and 100,000 (Milkov, 2000).

The porosity model summarized by Equation 1 assumes that compaction exponentially increases with depth, but it should be noted that mineral grain type, temperature, submarine landslides, presence of gas hydrates, mineral precipitation, and proximity of tectonic activity are among the variables that could cause deviation from this simple, smoothly varying porosity. The estimate of the total pore-water volume presented here was calculated regardless of fluid mobility or pore interconnectivity. Moreover, the minimum porosity at great depths, beyond which mechanical compaction stops, is unconstrained on a global scale and strongly varies with lithology. The choice of a full compaction scheme used here, which neglects the minimum porosity, results in a lower estimate of the total pore-fluid volume for especially thick sediments.

CONCLUSIONS

Several global data sets were combined to map the global three-dimensional distribution of temperature in marine sediments. As a result, we have shown that ~52% of marine sediments are above 40 °C, and if 80 °C is the effective limit to deep life, then ~25% of marine sediments are uninhabitable. In addition, we have calculated a total marine sediment volume (3.01×10^8 km^3) and an average thickness (721 m). We have produced the first determination of the volume of free water residing in marine sediments (8.46×10^7 km^3), equivalent to ~6% of the world's oceans. The methods used to carry out the work described here can also be used to quantify temperature-dependent processes such as diffusion, reaction rates, and thermodynamic drive, with important ramifications for the preservation of geological proxies. The temperature distributions reported here can be used to interpret ongoing investigations into the size, structure, and activity levels of microorganisms in the deep biosphere.

ACKNOWLEDGMENTS

Financial assistance was provided by the Center for Dark Energy Biosphere Investigations (C-DEBI, OCE0939564), the NASA Astrobiology Institute–Life Underground (NAI-LU, NNA13AA92A), and the European Union Horizon 2020 research and innovation program under the Marie Skłodowska-Curie grant agreement 643052 (C-CASCADES, Carbon Cascades from Land to Ocean in the Anthropocene). This is C-DEBI contribution 350 and NAI-LU contribution 099. Thorough reviews from Jens Kallmeyer, Ivano Aiello, and an anonymous reviewer have significantly improved this contribution.

REFERENCES CITED

Aagaard, P., and Helgeson, H.C., 1983, Activity/composition relations among silicates and aqueous solutions: II. Chemical and thermodynamic consequences of ideal mixing of atoms on homologous sites in montmorillonites, illites and mixed-layer clays: Clays and Clay Minerals, v. 31, p. 207–217, doi:10.1346/CCMN.1983.0310306.

Athy, L.F., 1930, Density, porosity and compaction of sedimentary rocks: American Association of Petroleum Geologists Bulletin, v. 14, p. 1–24.

Barnier, G.N., et al., 2006, Impact of partial steps and momentum advection schemes in a global ocean circulation model at eddy-permitting resolutions: Ocean Dynamics, v. 56, p. 543–567, doi:10.1007/s10236-006-0082-1 (erratum available at http://dx.doi.org/10.1007/s10236-009-0180-y).

Castelli, V.J., Stanley, E.M., and Fischer, E.C., 1974, The thermal conductivity of seawater as a function of pressure and temperature: Deep-Sea Research, v. 21, p. 311–319, doi:10.1016/0011-7471(74)90102-8.

Deyhle, A., and Kopf, A., 2001, Deep fluids and ancient pore waters at the backstop: Stable isotope systematics (C, B, O) of mud volcano deposits on the Mediterranean Ridge accretionary wedge: Geology, v. 29, p. 1031–1034, doi:10.1130/0091-7613(2001)029<1031:DFAAPW>2.0.CO;2.

Dimitrov, L.I., 2002, Mud volcanoes—The most important pathway for degassing deeply buried sediments: Earth-Science Reviews, v. 59, p. 49–76, doi:10.1016/S0012-8252(02)00069-7.

Divins, D.L., 2003, Total sediment thickness of the world's oceans & marginal seas: Boulder, Colorado, National Oceanic and Atmospheric Administration National Geophysical Data Center, https://www.ngdc.noaa.gov/mgg/sedthick/sedthick.html.

Eakins, B.W., and Sharman, G.F., 2010, Volumes of the world's oceans from ETOPO1: Boulder, Colorado, National Oceanic and Atmospheric Administration National Geophysical Data Center, https://www.ngdc.noaa.gov/mgg/global/etopo1_ocean_volumes.html.

Emerson, S., and Bender, M., 1981, Carbon fluxes at the sediment-water interface of the deep-sea—Calcium carbonate preservation: Journal of Marine Research, v. 39, p. 139–162.

Fowler, C.M.R., 1990, The solid Earth: An introduction to global geophysics: Cambridge, UK, Cambridge University Press, 728 p.

Fuchs, S., Schütz, F., Förster, H.-J., and Förster, A., 2013, Evaluation of common mixing models for calculating bulk thermal conductivity of sedimentary rocks: Correction charts and new conversion equations: Geothermics, v. 47, p. 40–52, doi:10.1016/j.geothermics.2013.02.002.

Hamza, V.M., Cardoso, R.R., and Ponte Neto, C.F., 2008, Spherical harmonic analysis of Earth's conductive heat flow: International Journal of Earth Sciences, v. 97, p. 205–226, doi:10.1007/s00531-007-0254-3.

Hantschel, T., and Kauerauf, A.I., 2009, Fundamentals of basin and petroleum systems modeling: Berlin, Springer-Verlag, 476 p.

Harder, J., 1997, Species-independent maintenance energy and natural population sizes: FEMS Microbiology Ecology, v. 23, p. 39–44, doi:10.1111/j.1574-6941.1997.tb00389.x.

Head, I.M., Gray, N.D., and Larter, S.R., 2014, Life in the slow lane; biogeochemistry of biodegraded petroleum containing reservoirs and implication for energy recovery and carbon management: Frontiers in Microbiology, v. 5, 566, doi:10.3389/fmicb.2014.00566.

Horsfield, B., et al., 2006, Living microbial ecosystems within the active zone of catagenesis: Implication for feeding the deep biosphere: Earth and Planetary Science Letters, v. 246, p. 55–69, doi:10.1016/j.epsl.2006.03.040.

Johnson, H.P., and Pruis, M.J., 2003, Fluxes of fluid and heat from the oceanic crustal reservoir: Earth and Planetary Science Letters, v. 216, p. 565–574, doi:10.1016/S0012-821X(03)00545-4.

Jørgensen, B.B., 1982, Mineralization of organic matter in the sea bed—The role of sulfate reduction: Nature, v. 296, p. 643–645, doi:10.1038/296643a0.

Kastner, M., Elderfield, H., and Martin, J.B., 1991, Fluids in convergent margins: What do we know about their composition, origin, role in diagenesis and importance for oceanic chemical fluxes?: Royal Society of London Philosophical Transactions, ser. A, v. 335, p. 243–259, doi:10.1098/rsta.1991.0045.

Kennett, J.P., 1982, Marine geology: Englewood Cliffs, New Jersey, Prentice Hall, 813 p.

Laske, G., and Masters, G., 1997, A global digital map of sediment thickness: Eos (American Geophysical Union Transactions), v. 78, p. F483.

Lipp, J.S., Morono, Y., Inagaki, F., and Hinrichs, K.-U., 2008, Significant contribution of Archaea to extant biomass in marine subsurface sediments: Nature, v. 454, p. 991–994, doi:10.1038/nature07174.

Milkov, A.V., 2000, Worldwide distribution of submarine mud volcanoes and associated gas hydrates: Marine Geology, v. 167, p. 29–42, doi:10.1016/S0025-3227(00)00022-0.

Prothero, D.R., and Schwab, F., 2004, Sedimentary geology: An introduction to sedimentary rocks and stratigraphy (second edition): New York, W.H. Freeman and Company, 557 p.

Ransom, B., and Helgeson, H.C., 1995, A chemical and thermodynamic model of dioctahedral 2:1 layer clay minerals in diagenetic processes: Dehydration of dioctahedral aluminous smectite as a function of temperature and depth in sedimentary basins: American Journal of Science, v. 295, p. 245–281, doi:10.2475/ajs.295.3.245.

Röling, W.F.M., Head, I.M., and Larter, S.R., 2003, The microbiology of hydrocarbon degradation in subsurface petroleum reservoirs: Perspectives and prospects: Research in Microbiology, v. 154, p. 321–328, doi:10.1016/S0923-2508(03)00086-X.

Shiklomanov, I.A., 1993, World fresh water resources, *in* Gleick, P.H., ed., Water in crisis: A guide to the world's fresh water resources: New York, Oxford University Press, p. 13–23.

Takai, K., Nakamura, K., Toki, T., Tsunogai, U., Miyazaki, M., Miyazaki, J., Hirayama, H., Nakagawa, S., Nunoura, T., and Horikoshi, K., 2008, Cell proliferation at 122°C and isotopically heavy CH_4 production by a hyperthermophilic methanogen under high-pressure cultivation: National Academy of Sciences Proceedings, v. 105, p. 10,949–10,954, doi:10.1073/pnas.0712334105.

Tissot, B.P., and Welte, D.H., 1984, Petroleum formation and occurrence: Berlin, Springer-Verlag, 699 p., doi:10.1007/978-3-642-87813-8.

Van Cappellen, P., and Wang, Y., 1996, Cycling of iron and manganese in surface sediments: A general theory for the coupled transport and reaction of carbon, oxygen, nitrogen, sulfur, iron and manganese: American Journal of Science, v. 296, p. 197–243, doi:10.2475/ajs.296.3.197.

Vion, A., and Menot, L., 2009, Continental margins between 140m and 3500m depth: IFREMER, http://www.marineregions.org/ (July 2015).

Walker, J.C.G., Hays, P.B., and Kasting, J.F., 1981, A negative feedback mechanism for the long-term stabilization of Earth's surface temperature: Journal of Geophysical Research, v. 86, p. 9776–9782, doi:10.1029/JC086iC10p09776.

Wallmann, K., Pinero, E., Burwicz, E.B., Haeckel, M., Hensen, C., Dale, A.W., and Ruepke, L., 2012, The global inventory of methane hydrate in marine sediments: A theoretical approach: Energies, v. 5, p. 2449–2498, doi:10.3390/en5072449.

Whittaker, J.M., Goncharov, A., Williams, S.E., Dietmar Müller, R., and Leitchenkov, G., 2013, Global sediment thickness set updated for the Australian-Antarctic Southern Ocean: Geochemistry, Geophysics, Geosystems, v. 14, p. 3297–3305, doi:10.1002/ggge.20181.

Wilhelms, A., Larter, S.R., Head, I., Farrimond, P., di-Primio, R., and Zwach, C., 2001, Biodegradation of oil in uplifted basins prevented by deep-burial sterilization: Nature, v. 411, p. 1034–1037, doi:10.1038/35082535.

Zonneveld, K.A.F., et al., 2010, Selective preservation of organic matter in marine environments; processes and impact on the sedimentary record: Biogeosciences, v. 7, p. 483–511, doi:10.5194/bg-7-483-2010.

Manuscript received 14 September 2016
Revised manuscript received 1 December 2016
Manuscript accepted 2 December 2016

Printed in USA